EPJ A
Hadrons and Nuclei

EPJ.org
your physics journal

Eur. Phys. J. A (2011) 47: 126 DOI 10.1140/epja/i2011-11126-0

Cluster pre-existence probability

N.S. Rajeswari, K.R. Vijayaraghavan and M. Balasubramaniam

Società Italiana di Fisica

Springer

Eur. Phys. J. A (2011) **47**: 126
DOI 10.1140/epja/i2011-11126-0

THE EUROPEAN PHYSICAL JOURNAL A

Regular Article – Theoretical Physics

Cluster pre-existence probability

N.S. Rajeswari, K.R. Vijayaraghavan and M. Balasubramaniam[a]

Department of Physics, Bharathiar University, Coimbatore - 641046, India

Received: 1 August 2011 / Revised: 20 September 2011
Published online: 24 October 2011 – © Società Italiana di Fisica / Springer-Verlag 2011
Communicated by M. Hjorth-Jensen

Abstract. Pre-existence probability of the fragments for the complete binary spectrum of different systems such as ^{56}Ni, ^{116}Ba, ^{226}Ra and ^{256}Fm are calculated, from the overlapping part of the interaction potential using the WKB approximation. The role of reduced mass as well as the classical hydrodynamical mass in the WKB method is analysed. Within WKB, even for negative Q-value systems, the pre-existence probability is calculated. The calculations reveal rich structural information. The calculated results are compared with the values of preformed cluster model of Gupta and collaborators. The mass asymmetry motion is shown here for the first time as a part of relative separation motion.

1 Introduction

Spontaneous decay of radioactive nuclei via emission of heavy ions, *i.e.* nuclei heavier than the α particle, generally called as clusters, which was theoretically predicted by Sandulescu *et al.* [1] and later experimentally confirmed by Rose and Jones [2], is now a well-established phenomenon [3–12]. Such cluster emission from the excited light- and medium-mass parent nuclei produced in low-energy nuclear reactions has also attracted much interest recently [13–20]. Cluster emission could be considered either as a case of asymmetric fission or as a two-step process of preformation and/or pre-existence of cluster and then decay from the parent nucleus by impinging on the confining barrier, similar to α decay. In models based on the former case, also called unified fission models (UFM), the pre-existence probability of the emitted cluster is considered to be equal to one. In the later approach referring to preformed cluster models (PCM) the cluster decay process is considered to be happening in two stages. In the first stage it is assumed that the cluster, which is to be emitted by the radioactive parent nucleus, is already preborn inside it. In the second stage this cluster crosses the interaction barrier with a tunnelling probability. In these models the cluster pre-existence probability depends on the size of the emitted cluster. In general this probability can be calculated either empirically or theoretically. An empirical pre-existence probability of a cluster is defined simply as a measure of disagreement between theoretical calculation and experimental data of cluster decay constant or half-lives. In theoretical estimates, the pre-existence probabilities of clusters are estimated based on either single particle picture (shell model), or on collective model picture. The model due to Blendowske *et al.* [6–8] uses a shell model approach for the many-body wave function and defines the pre-existence probability and/or spectroscopic factor as the probability of finding the decay channel space in the parent nucleus wave function. Using microscopic wave functions, they have calculated the probability for finding the ^{14}C daughter nucleus structure in Ra nucleus. The pre-existence probability is found to possess a simple mass dependence on the emitted cluster [6–8]. These microscopic calculations are limited only to light clusters upto $A_2 \leq 16$. These authors have later introduced an empirical expression for pre-existence probability that fits their microscopically calculated spectroscopic factors for ^{4}He, ^{12}C, ^{14}C and ^{16}O. In collective model picture, the preformation probability is calculated by solving the Schrödinger equation of motion in mass and charge asymmetry coordinates and is essentially based on the nuclear-structure information of the decay process. The model due to Gupta and co-workers [11,12] defines the quantum-mechanical preformation probability of finding the fragments A_1 and A_2 (with fixed charges Z_1 and Z_2, respectively) through the dynamical collective coordinate of mass and charge asymmetries of the decay products as

$$\eta = \frac{A_1 - A_2}{A}, \qquad \eta_Z = \frac{Z_1 - Z_2}{Z}, \tag{1}$$

at relative separation R (fixed at touching configuration) of the decay path.

By solving the stationary Schrödinger equation,

$$\left[-\frac{\hbar^2}{2\sqrt{B_{\eta\eta}}}\frac{\partial}{\partial\eta}\frac{1}{\sqrt{B_{\eta\eta}}}\frac{\partial}{\partial\eta} + V(\eta)\right]\psi^\nu(\eta) = E^\nu_\eta \psi^\nu(\eta), \tag{2}$$

numerically, $|\psi^\nu(\eta)|^2$ gives the probability of finding the mass fragmentation η at a fixed position R on the decay

[a] e-mail: m.balou@gmail.com

path. Normalising and scaling $|\psi(\eta)|^2$ to give the fractional mass yield at, say, the mass A_2 of the cluster ($\mathrm{d}\eta = 2/A$), the cluster preformation probability, for the ground-state decay is given as

$$P_0(A_2) = |\psi(\eta)|^2 \sqrt{B_{\eta\eta}(\eta)} \left(\frac{2}{A}\right). \quad (3)$$

Though the PCM and UFM differ in the concept, both of these approaches produce similar results for explaining the exotic cluster decay process. This may be understood by the interpretation of Poenaru and Greiner [21, 22] that the cluster preformation probability considered in PCM is equivalent to the penetrability of the inner barrier (overlapping region) from the parent nucleus radius to the touching configuration of cluster and daughter (*i.e.* the overlapping region of fragments), within the unified fission model. The difference between an UFM and a PCM appears in the expression for the decay constant:

$$\lambda_{UFM} = \nu_0 P, \quad \lambda_{PCM} = \nu_0 P P_0, \quad (4)$$

where ν_0 is the frequency of assaults on the barrier, P is barrier penetrability and P_0 is the preformation probability.

According to the interpretation of Poenaru *et al.*, in unified fission models, the penetrability P could be expressed as a product of two terms as $P = P_{ov}\ P_{nov}$. Here P_{ov} corresponds to the inner part of the barrier (overlapping or pre-touching stage) and is calculated by evaluating the WKB integral with the limits from the radius of the parent nucleus (R_0) to touching configuration (R_t) and P_{nov} corresponds to the post-touching configuration. In this work, taking the idea of Poenaru and Greiner, we have estimated the pre-existence probability values of entire binary fragmentation of four nuclei *viz.*, ^{56}Ni, ^{116}Ba, ^{226}Ra and ^{256}Fm from different mass regions. The calculated results are compared with the preformation probabilities obtained from PCM. The methodology is briefly described in the following section and the results and discussions are presented in sect. 3.

2 The methodology

In PCM of Gupta and co-workers, the potential energy of the overlapping region is considered as a second-order polynomial of the form

$$V(R) = a_1 R + a_2 R^2 \quad \text{for} \quad R_0 \le R \le R_t, \quad (5)$$

with R as the relative separation between the centres of the two emitted nuclei. For the post-touching region, the potential is simply the sum of Coulomb and proximity potentials as given by

$$V(R) = \frac{Z_1 Z_2 e^2}{R} + V_p \quad \text{for} \quad R_t \le R \le R_b, \quad (6)$$

where Z_i's are the charge numbers of the fragments (with $i = 1$ and 2) and $e^2 = 1.44$ MeV fm. Such potential for the fragmentation of a parent nucleus A into two fragments A_1 and A_2 is shown in fig. 1. In this figure, the solid line corresponds to the the actual potential calculated using eq. (6). From R_0 to R_t, the potential is simply a polynomial as defined in eq. (5) connecting to Q-value at R_0, shown here by dotted line. In order to calculate barrier penetration probability, the Q-value should be a positive quantity. But when one considers the entire binary fragmentation of nuclei from different mass regions, several mass asymmetries may have a negative Q-value. In order to calculate the pre-existence probability for entire binary spectrum, through barrier penetrability integral, the Q-values should be scaled so as to have positive value; such potential is shown in fig. 1 by dashed lines, scaled by an arbitrary amount of 25 MeV to make the Q-values a positive quantity denoted here by Q'. (For a particular nucleus, this arbitrary amount depends on the minimum Q value in the Q-value spectrum corresponding to all the charge minimized mass asymmetries.) Thus, the overlapping integral (defined later) of scaled potential would give pre-existence probability for the negative Q-value. In eq. (6),

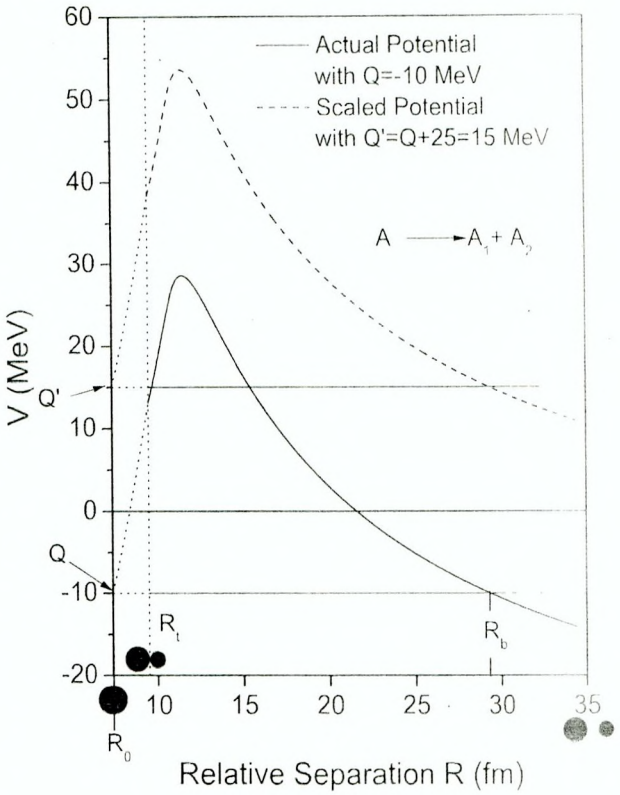

Fig. 1. A general negative Q-value scattering potential for the fragmentation of A into A_1 and A_2. From touching configuration onwards the actual and scaled potentials are plotted as solid line and dashed line, respectively. In both cases the overlapping region is shown by dotted lines. The turning points R_0, R_t and R_b and actual and scaled Q-values are labelled.

the proximity potential V_p is due to Blocki *et al.* [23] and is given by

$$V_p = 4\pi\overline{R}\gamma b\Phi(\xi). \tag{7}$$

$\Phi(\xi)$ is the universal function of proximity potential, which depends only on the distance between two nuclei and is independent of the charge numbers of the two nuclei, given as

$$\Phi(\xi) = \begin{cases} -\frac{1}{2}(\xi - 2.54)^2 - 0.0852(\xi - 2.54)^3, & \xi \leq 1.251, \\ -3.437\exp(-\frac{\xi}{0.75}), & \xi \geq 1.251. \end{cases} \tag{8}$$

Here, $\xi = s/b$. This function is defined for negative (the overlapping region), zero (touching configuration) and positive values of s. $b \sim 1$ fm is the diffuseness of the nuclear surface. The γ is the specific nuclear surface tension coefficient given by

$$\gamma = 0.9517\left[1 - 1.7826\left(\frac{N-Z}{A}\right)^2\right] \text{MeV fm}^{-2}, \tag{9}$$

$\overline{R}$ is the mean curvature radius of the reaction partners, characterising the gap, which for spherical nuclei is given by

$$\overline{R} = \frac{C_1 C_2}{C_1 + C_2} \text{ fm}. \tag{10}$$

The potential $V(R)$ is calculated at R_t for fixed η. R_t is defined as $R_t = C_1 + C_2$, and here, $C_i (i = 1, 2)$ are the Süssman's central radii and are related to the effective sharp radii $R_i = 1.28A_i^{1/3} - 0.76 + 0.8A_i^{-1/3}$ fm, as

$$C_i = R_i\left(1 - \frac{b^2}{R_i^2}\right) \text{ fm}. \tag{11}$$

For the decay constant defined for UFM in eq. (4), the total penetration probability is $P = P_{ov}P_{nov}$. The overlapping penetration probability (P_{ov}) is given by

$$P_{ov} = \exp\left[-\frac{2}{\hbar}\int_{R_0}^{R_t}\{2\mu[V(R) - Q]\}^{1/2}\mathrm{d}R\right]. \tag{12}$$

Here R_0 and R_t are the first and second turning points, respectively. The tunnelling probability between these two turning points gives the pre-existence probability within WKB approximation. The total penetration probability (P) is given by,

$$P = \exp\left[-\frac{2}{\hbar}\int_{R_0}^{R_b}\{2\mu[V(R) - Q]\}^{1/2}\mathrm{d}R\right]. \tag{13}$$

Here R_0 and R_b are the first and second turning points, respectively. The second turning point is calculated from the condition $R_b = Z_1Z_2e^2/Q$. This means that the tunnelling begins at $R = R_0$ and terminates at $R = R_b$, with $V(R_b) = Q$-value of the ground-state decay. In the above integrals, $\mu = \frac{A_1A_2}{A_1+A_2}m$ is the reduced mass with m being the nucleon mass.

It is to be mentioned here that in PCM, while calculating the preformation probability as defined in eq. (3), the masses used in the kinetic energy of the Schrödinger equation are the classical hydrodynamical masses $B_{\eta\eta}$ of Kröger and Scheid [24] defined by

$$B_{\eta\eta} = \frac{AmR^2}{4}\left[\frac{v_t(1+\beta)}{v_c(1+\delta^2)} - 1\right], \tag{14}$$

with

$$\beta = \frac{R_c}{2R}\left[\frac{1}{1+\cos\theta_1}\left(1 - \frac{R_c}{R_1}\right) + \frac{1}{1+\cos\theta_2}\left(1 - \frac{R_c}{R_2}\right)\right], \tag{15}$$

$$\delta = \frac{1}{2R}\left[(1-\cos\theta_1)(R_1 - R_c) + (1-\cos\theta_2)(R_2 - R_c)\right], \tag{16}$$

$$v_c = \pi R_c^2 R, \tag{17}$$

and $v_t = v_1 + v_2$, the total conserved volume. R_c is the radius of a cylinder of length R, having a homogeneous flow in it, whose existence is assumed for the mass transfer between the two spherical fragments. The flow is assumed to be radial. The authors use a special ansatz for R_c:

$$R_c = \alpha\ \min(R_1, R_2)\ f(\frac{R}{R_t}) \tag{18}$$

with

$$f(x) = 1 \qquad \text{if } x \leq 1, \tag{19}$$

and α-values from 0.4 to 0.8 are shown to have best fit with the microscopic calculations. In PCM calculations, we use $\alpha = 0.4$. The $B_{\eta\eta}$ is in MeV fm^2. The geometry of the model is also given in ref. [24].

In order to have a direct comparison between the pre-existence probability calculated using eq. (12) with that of PCM calculations, we have performed calculations using both the reduced mass and hydrodynamical mass in the WKB integrals denoted, respectively, as $P_{ov}(\mu)$ and $P_{ov}(B_{\eta\eta})$. However, while using hydrodynamical mass in the WKB integral in order to have proper cancellation of units for the probability, we divide the value of $B_{\eta\eta}$ by R^2 on both sides of eq. (14) which gives rise to a quantity which we term here as reduced hydrodynamical mass. Further, it is to be mentioned here that, in PCM also, the preformation probabilites are calculated at a constant R value, say at touching configuration. Hence, reduced $B_{\eta\eta}$ values will not change the structural information. In other words, the $B_{\eta\eta}$ values are reduced by an amount of R^2. Furhter the preformation probabilities P_0 in PCM and the pre-existence probabilities calculated for the use of $P_{ov}(\mu)$ and $P_{ov}(B_{\eta\eta})$ are all normalized to one and hence the results are comparable with each other. The results obtained are presented in the following section.

3 Results and discussions

For the first time the mass asymmetry motion for the complete binary spectrum is shown here as a part of the relative separation motion. The calculations are made for four

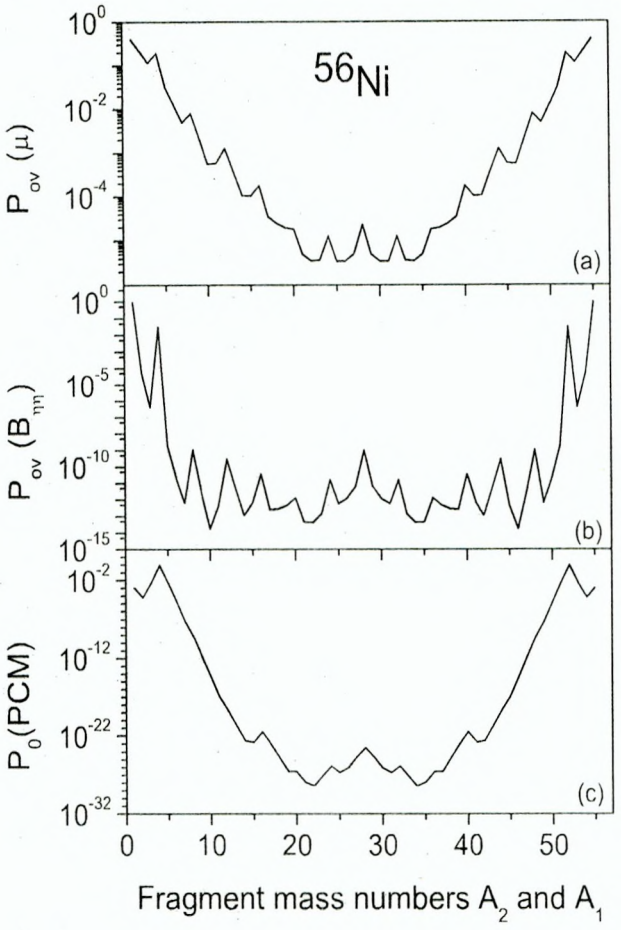

Fig. 2. Panels (a) and (b): The overlapping pre-existence probability plotted as a function of fragment mass numbers A_1 and A_2 of all the binary fragmentation of ^{56}Ni for the use of reduced mass and hydrodynamical mass, respectively. The Q-values of all mass asymmetries are scaled by 27 MeV. Panel (c): The preformation probability calculated within preformed cluster model [12] for the use of hydrodynamical mass.

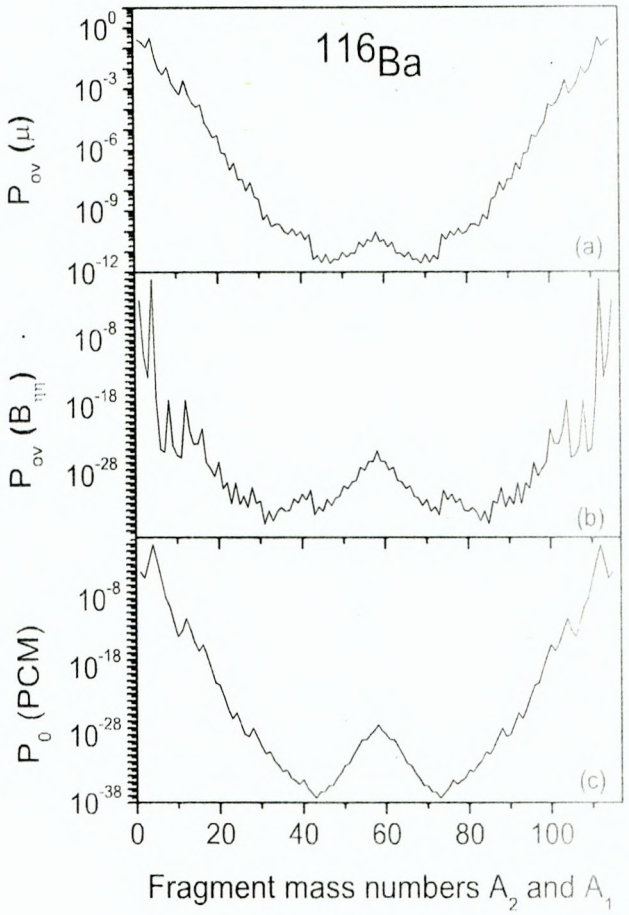

Fig. 3. Same as fig. 2 but for ^{116}Ba. In panels (a) and (b), the Q-values of all mass asymmetries are scaled by 22 MeV.

different nuclei from different mass regions just to validate the method. Some preliminary results obtained for ^{56}Ni was presented in ref. [25]. Within WKB approximation, in order to calculate the pre-existence probability, the minimum requirement is that the Q-value should be a positive quantity. However, if one considers the complete binary spectrum of ^{56}Ni, the Q-values are negative for all the charge minimized mass asymmetries and further for cases like ^{116}Ba, ^{226}Ra and ^{256}Fm the Q-values are negative for at least few mass asymmetries. Hence in order to make all the Q-values a positive quantity, the entire Q-values corresponding to all the charge minimized mass asymmetries are scaled by a uniform amount. In the case of ^{56}Ni the Q-value of all the charge minimized mass asymmetries ranges from −25.7463 MeV to −6.769 MeV. The scaling amount used is 27 MeV which makes the scaled Q-values ranging from 1.2537 MeV to 20.231 MeV. It means all the Q-values are scaled uniformly making them a positive quantity. Even for any other value greater than 27 MeV taken uniformly throughout, the end result will not change. The same amount of scaling is applied to the potential making the area under the potential the same for negative Q-value case as well as scaled Q-value case. Figure 4 represents one such case showing actual negative Q-value and scaled Q-value. In both cases the area under the curve will remain the same after appropriate scaling. Similarly for the cases of ^{116}Ba, ^{226}Ra and ^{256}Fm, we have chosen the scaling amount as 22 MeV, 17 MeV and 17 MeV, respectively, to make the Q-value spectrum a positive quantity (the potential is also scaled uniformly by this amount). Since different scaling amount applied uniformly would give same results, it is not shown explicitly. In figs. 2(a) and (b), the pre-existence probability of all the exit channels of ^{56}Ni nucleus, calculated using reduced as well as hydrodynamical masses in eq. (12) is shown as a function of fragment mass numbers A_1 and A_2. (For the hydrodynamical case, the α-value is taken as 0.4.) It is seen that in both cases the probability decreases with increase in

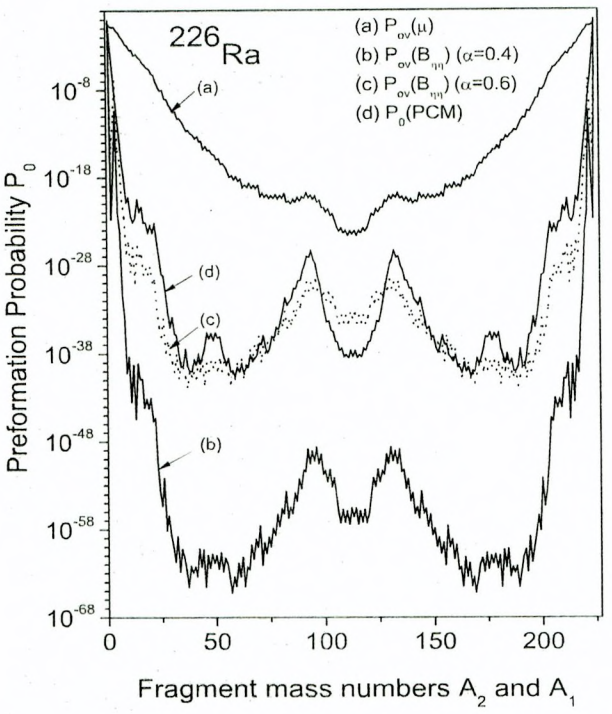

Fig. 4. The overlapping pre-existence probability plotted as a function of fragment mass numbers A_1 and A_2 of all the binary fragmentation of ^{226}Ra (a) for the use of reduced mass and (b) and (c) for hydrodynamical mass with values of $\alpha = 0.4$ and 0.6, respectively. (d) The preformation probability calculated within preformed cluster model [12] for the use of hydrodynamical mass. In (a), (b) and (c) the Q-values of all mass asymmetries are scaled by 17 MeV.

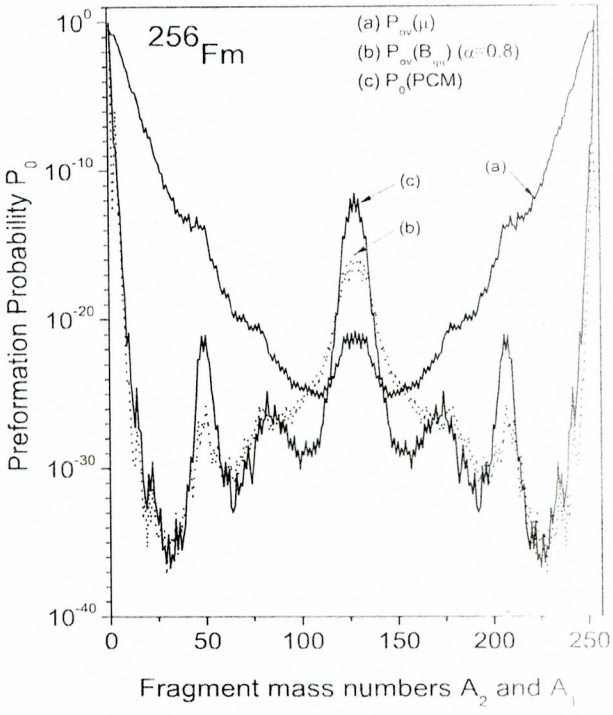

Fig. 5. The overlapping pre-existence probability plotted as a function of fragment mass numbers A_1 and A_2 of all the binary fragmentation of ^{256}Fm (a) for the use of reduced mass and (b) for the use of hydrodynamical mass with $\alpha = 0.8$. (c) The preformation probability calculated within preformed cluster model [12] for the use of hydrodynamical mass. In (a) and (b) the Q-values of all mass asymmetries are scaled by 17 MeV.

size of the cluster and there are prominently larger values for the α-structured nuclei. Though the structural variations are similar in both cases but with reduced mass the pre-existence probability is higher as compared to hydrodynamical mass calculations. It is to be mentioned here that ^{56}Ni* formed in low-energy reactions is shown to have higher cross-sections for the α-structured nuclei in the exit channel. The ground-state pre-existence probability thus obtained here clearly support a four nucleon transfer mechanism. The effect of temperature in the scattering potential will only change the scale of potential but the same structure will persist. Figure 2(c) presents the preformation probability calculated within PCM for hydrodynamical masses. The PCM calculations show a strong peak at ^{4}He and then the probability decreases rapidly showing a shoulder at ^{12}C and a small peak at ^{16}O. The magnitude of preformation probability as calculated in WKB approximation for the use of reduced and hydrodynamical masses and PCM calculation is not comparable. However, the calculations of WKB approximation show an excellent structure effect.

Like ^{56}Ni*, another such system studied extensively recently is ^{116}Ba* formed in low-energy reactions. The emission of complex intermediate mass fragments is shown to be predominant from the excited ^{116}Ba*. This mass region was expected to be a fertile region to observe spontaneous cluster emission associated with closed shell Sn nucleus. Though theoretically predicted as a fertile region to observe cluster decay, the experimental attempts ended only with upper limits steering the direction to study such emission from excited systems in this mass region. In figs. 3(a) and (b) we present the pre-existence probability $P_{ov}(\mu)$ and $P_{ov}(B_{\eta\eta})$, respectively of ^{116}Ba. The Q values of some of the asymmetric channels are negative, hence the potential is scaled by 22 MeV for all the exit channels to make all the Q-values positive as mentioned earlier. It is interesting to note that the four-nucleon transfer mechanism in the pre-existence is evident in both cases. Particularly in fig. 3(a), peaking at alpha-structured nuclei occurs at least up to ^{28}Si and beyond that the structural variation is simply due to odd-even effect. In fig. 3(b) there is prominent peak at ^{4}He and noticeable peaks at ^{8}Be, ^{12}C, ^{16}O and ^{20}Ne and afterwards the probability is

higher for even fragments. Comparing the magnitude of both of these cases, for the use of hydrodynamical mass (with $\alpha = 0.4$) the magnitude of the pre-existence probability is relatively smaller. However, it compares well with the PCM calculations as presented in fig. 3(c). The WKB calculations again show an excellent structure effect.

In fig. 4, for the case of ^{226}Ra since the magnitude of the overlapping pre-existence probabilities ($P_{ov}(\mu)$ and $P_{ov}(B_{\eta\eta})$) are comparable with the magnitude of preformation probability calculated using PCM, the results are presented in a single panel. ^{226}Ra is a known cluster emitter. Hence the structural variation in the pre-existence probability is of importance. In this figure we present also the role of the parameter α entering the calculations for the use of hydrodynamical masses. In this figure, the line marked with (a) corresponds to the $P_{ov}(\mu)$ and the line marked with (b) and (c) corresponds to $P_{ov}(B_{\eta\eta})$ for the use of $\alpha = 0.4$ and 0.6, respectively. The line (c) is plotted as a dotted line just to distinguish it from line (d). The preformation probability calculated in PCM is shown by line (d). The calculations with reduced mass do not show much structural variation except for a small peaking around near symmetric region, whereas the calculations with hydrodynamical mass clearly show, peaks around ^{14}C as well as near Mg and Si. The magnitude of calculations with hydrodynamical mass for $\alpha = 0.4$ lies far below than that of the PCM calculations however by changing the α-value as 0.6 closely matches with PCM calculations. It is to be mentioned here that, in PCM calculations α-value is taken always as 0.4.

For binary decay of ^{256}Fm, all the exit channel potentials are scaled uniformly by an amount of 17 MeV to make all the Q-values a positive quantity. This system is a good case corresponding to single humped mass distribution in the fission yields. The calculated pre-existence probabilities are presented in fig. 5. In this figure, the line marked with (a) corresponds to the $P_{ov}(\mu)$ and the line marked with (b) corresponds to $P_{ov}(B_{\eta\eta})$ for the use of $\alpha = 0.8$. The preformation probability calculated in PCM is shown by line (c). All the three calculations clearly show a single humped distribution the magnitude of which is greater in PCM calculations. The WKB calculations with hydrodynamical mass clearly exhibit similar structural variation with that of PCM calculations. But the WKB calculations with reduced mass monotonically decreases with increase in mass number except near the symmetric region.

In the calculations presented for different cases, the difference in magnitude is due to the different mass parameters we use in the calculations. For the use of reduced mass in the WKB integral, at least for lighter systems like ^{56}Ni and ^{116}Ba, the structural variation resembles that of PCM calculations but for the heavier systems like ^{226}Ra and ^{256}Fm the structure is different from that of PCM calculations. However, if one uses reduced hydrodynamical mass in place of reduced mass in the WKB integral, we get a remarkable similar structural variation with that of PCM calculations. Further, this result can be fine-tuned with the parameter α to change the magnitude as well.

4 Summary

Summarizing, the pre-existence probability of systems ^{56}Ni, ^{116}Ba, ^{226}Ra and ^{256}Fm are calculated, for the overlapping part of the potential, using the idea suggested by Poenaru *et al.*, using WKB integral. The pre-existence probability within WKB method is obtained for the use of reduced mass as well as classical hydrodynamical mass. Even for negative Q-value systems, the pre-existence probability is calculated within WKB method by scaling the Q value and the potentials to make them a positive quantity. The calculated results are compared with the results of the preformed cluster model (PCM) of Gupta and collaborators. The WKB calculations with reduced mass show structural variation corresponding to four-nucleon transfer for the complete spectrum of ^{56}Ni and at least up to ^{20}O corresponding to ^{116}Ba. For heavy systems like ^{226}Ra and ^{256}Fm, these calculations do not show strong structural variations. However, the WKB calculations with hydrodynamical mass show strong structural variations for all the cases considered and in particular for heavier systems the results obtained are similar to PCM calculations. Further, the magnitude of pre-existence probability using hydrodynamical mass in WKB method can be closer to the PCM results by varying the value of the parameter α entering the calculations of hydrodynamical mass. The mass asymmetry motion is shown as a part of the relative separation motion.

One of the authors MB acknowledges the financial support in the form of project sanctioned to him by the University Grants Commission of India, vide letter No.37-100/(2009). NSR acknolwedges the support in the form of study leave granted by Avinashilingam Institute for Home Science and Higher Education for women, Coimbatore.

References

1. A. Săndulescu, D.N. Poenaru, W. Greiner, Sovt. J. Part. Nucl. **11**, 528 (1980).
2. H.J. Rose, G.A. Jones, Nature **307**, 245 (1984).
3. Y.J. Shi, W.J. Swiatecki, Phys. Rev. Lett. **54**, 300 (1985).
4. G.A. Pik-Pichak, Sovt. J. Nucl. Phys. **44**, 923 (1986).
5. M. Irindo, D. Jerrestam, R.J. Liotta, Nucl. Phys. A **454**, 252 (1986).
6. R. Blendowske, T. Fliessbach, H. Walliser, Nucl. Phys. A **464**, 75 (1987).
7. R. Blendowske, H. Walliser, Phys. Rev. Lett. **61**, 1930 (1988).
8. R. Blendowske, T. Fliessbach, H. Walliser, Z. Phys. A **339**, 121 (1991).
9. G. Shanmugam, B. Kamalaharan, Phys. Rev. C **38**, 1377 (1988).
10. B. Buck, A.C. Merchant, J. Phys. G Nucl. Part. Phys. **15**, 615 (1989).
11. R.K. Gupta, *Proceedings of the 5th International Conference on Nuclear Reaction Mechanisms, Varenna, June 13-18, 1988*, edited by E. Gadioli, Ric. Sci. Suppl., No. 66 (1988) p. 416.
12. S.S. Malik, R.K. Gupta, Phys. Rev. C **39**, 1992 (1989).
13. S.J. Sanders, A. Szanto de Toledo, C. Beck, Phys. Rep **311**, 487 (1999).

14. M. La Commara, J. Gomez del Campo, A. D'Onofrio, A. Gadea, M. Glogowski, P. Jarillo-Herrero, N. Belcari, R. Borcea, G. de Angelis, C. Fahlander, M. Gòrska, H. Grawe, M. Hellström, R. Kirchner, M. Rejmund, V. Roca, E. Roeckl, M. Romano, K. Rykaczewski, K. Schmidt, Nucl. Phys. A **669**, 43 (2000).
15. R.K. Gupta, M. Balasubramaniam, C. Mazzocchi, M. La commara, W. Schied, Phys. Rev. C **65**, 024601 (2002).
16. R.K. Gupta, R. Kumar, N.K. Dhiman, M. Balasubramaniam, W. Schied, C. Beck, Phy. Rev. C **68**, 014610 (2003).
17. M. Balasubramaniam, R. Kumar, R.K. Gupta, C. Beck, W. Scheid, J. Phys. G Nucl. Part. Phys. **29**, 2703 (2003).
18. R.K. Gupta, M. Balasubramaniam, R. Kumar, D. Singh, C. Beck, Nucl. Phys. A **738**, 479 (2004).
19. R.K. Gupta, M. Balasubramaniam, R. Kumar, D. Singh, C. Beck, W. Greiner, Phys. Rev. C **71**, 014601 (2005).
20. R.K. Gupta, M. Balasubramaniam, R. Kumar, D. Singh, C. Beck, W. Greiner, J. Phys. G Nucl. Part. Phys. **32**, 345 (2006).
21. D.N. Poenaru, W. Greiner, J. Phys. G Nucl. Part. Phys. **17**, S443 (1991).
22. D.N. Poenaru, W. Greiner, Phys. Scripta **44**, 427 (1991).
23. J. Blocki, J. Randrup, W.J. Swiatecki, C.F. Tsang, Ann. Phys. (NY) **105**, 427 (1977).
24. H. Kröger, W. Scheid, J. Phys. G Nucl. Phys. **6**, 85 (1980).
25. N.S. Rajeswari, M. Balasubramaniam. *Proceedings of the DAE-BRNS Symposium on Nuclear Physics*, Vol. 55, 186 (2010).